Poster2-91 MULTI-SCALE STRUCTURE OF MESO-GAMMA SCALE VORTEX OBSERVED BY X-BAND DOPPLER RADARS

Hanako Y. Inoue*[1], Kenichi Kusunoki[1], Naoki Ishitsu[1], Ken-ichiro Arai[1], Chusei Fujiwara[2], Toru Adachi[1], and Hiroto Suzuki[2]

[1]Meteorological Research Institute, Tsukuba, Japan
[2]East Japan Railway Company, Saitama, Japan

1. INTRODUCTION

On 24 November 2017, a meso-gamma scale vortex (MGV) developed in the Japan sea coastal region. The MGV showed distinct structural change as it approached the coast, and many misovortices developed within the MGV, which was well observed by two X-band Doppler radars.

Japan sea coastal region is among the best-known locations for intense sea-effect snow events and various scales of mesoscale vortices have been documented (e.g., Asai 1988, Nagata 1993, Yanase et al. 2016, Watanabe et al. 2016). Mesoscale vortices have been documented in other parts of the world, such as the Great Lakes of North America (e.g., Laird et al. 2001; Grim et al. 2004). Although some studies have shown multi-scale structure of meso-alpha scale vortices (Tsuboki and Asai 2004), those of smaller vortices have not been understood well (Inoue et al. 2011).

To clarify the multi-scale structure of observed MGV, we performed single- and dual-Doppler radar analysis of two X-band Doppler radars.

2. OBSERVATION

We mainly used two X-band Doppler radars in the Shonai area, Yamagata Prefecture, Japan (Fig. 1). The Doppler radar of the East Japan Railway Company (RJRE) (Fujiwara et al. 2018), has a maximum observation range of 60 km, and its radial resolution is 75 m. Its beamwidth is 1.2°, and it observes low levels (0.6°, 0.9°) continuously in plan position indicator (PPI) mode at 4 rpm. The portable X-band Doppler radar (XPOD) of the Meteorological Research Institute has a maximum observational range of 24 km. Its radial resolution is 30 m, and its beamwidth is 2.0°. The XPOD was operated in multiple PPI modes (2°, 6°, 10°, 2°, 14°, and 18°) with updates every 1 minute and the range height indicator (RHI)(285°) with updates every 3.5 minutes.

We manually detected vortices by identifying a Doppler velocity maximum (V_{max}) and minimum (V_{min}) couplet and then tracked its size and location on each PPI scan. To estimate core diameter (D), peak tangential velocity (V_t), and vertical vorticity (ζ) of a misovortex from single-Doppler radar observation, we assumed a simple Rankine vortex. D was calculated by the distance between V_{max} and V_{min}, and V_t and ζ was calculated by

$$V_t=(V_{max}-V_{min})/2, \quad (1)$$

$$\zeta=4V_t/D, \quad (2)$$

For the estimation of D, V_t, ζ of MGV, we used a least-squares method based on Suzuki et al. (2007) and calculated best-fit Rankine vortex parameters (D, V_t, ζ) for observed MGV.

We also performed a dual-Doppler analysis to derive horizontal wind fields. The data were interpolated into a 100×100-m Cartesian grid using a Cressman-type weighting function. Horizontal wind fields were obtained by a standard dual-Doppler analysis based on Ishihara et al. (1986). We used RJRE 1°- and XPOD 2°-elevation-angle scan data to derive horizontal winds at 300 m ASL. Analyses were constrained to an area in which the radar-beam intersection angles are between 20° and 160°, and the altitude differences are less than 200 m (Fig. 1). The average moving speed of MGV was used to adjust the time differences between RJRE and XPOD scans.

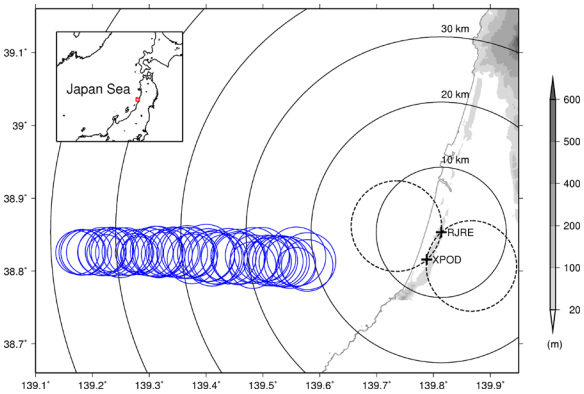

Fig. 1: Map showing locations of radars(crosses), distances from RJRE radar (concentric 10-km-interval contours), area of dual-Doppler analysis (dashed circles except overlapping part), and eastward track of MGV before its decay (blue circle). Terrain levels at 20, 100, 200, 300, 400, 500, 600 m ASL (gray shading) are also shown.

3. MULTI-SCALE STRUCTURE OF MGV

3.1 *Structural change of MGV*

MGV of 6-8 km diameter developed offshore under a winter monsoon situation, traveled eastward to the coast and approached the radars. The MGV

* *Corresponding author address:* Hanako Y. Inoue, Meteorological Research Institute, 1-1 Nagamine, Tsukuba, 305-0052, Japan; e-mail: hainoue@mri-jma.go.jp.

was first identified by a distinct Doppler velocity couplet with comma-shaped reflectivity pattern (Fig.2i). As the misovortices (less than 2km in diameters) developed within the MGV, MGV gradually decayed. Both Doppler velocity and reflectivity pattern became more complicated with small-scale velocity couplets and accompanying kinks (Fig. 2ii, iii).

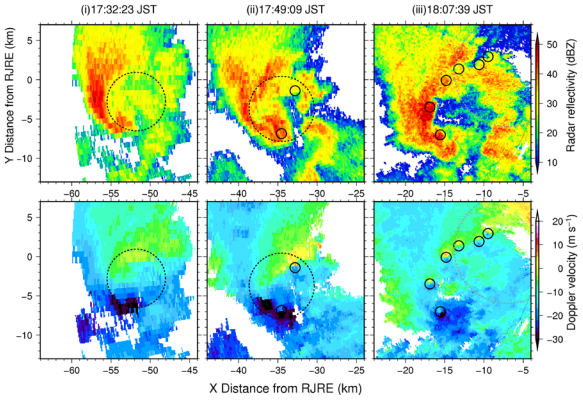

Fig. 2: PPI images of (top) reflectivity and (bottom)Doppler velocity observed by RJRE at elevation of 1.0° at (i) 17:32:23 JST, (ii) 17:49:09, and (iii) 18:07:39 JST. Also shown are the area of dual-Doppler analysis (dashed gray circle), MGV (dashed circle), misovortices (small circles), and coastline (solid gray line).

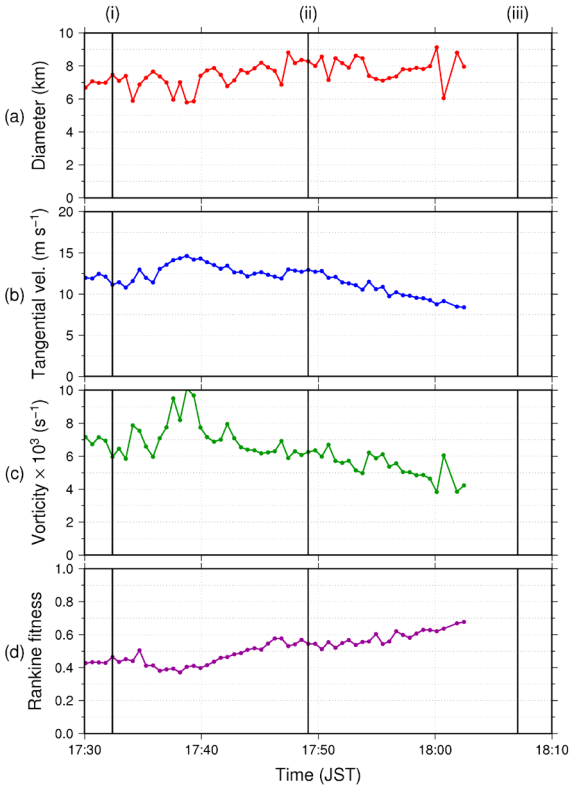

Fig. 3: Temporal change of (a) D, (b) V_t, (c) ζ, and (d) Rankine fitness parameter of MGV derived from RJRE observations. The solid vertical lines labeled i to iii correspond to panels (i) to (iii) in Fig. 2.

We investigated the temporal change of MGV from single-Doppler analysis of RJRE (Fig. 3). From 17:30 JST to 17:40 JST, V_t and ζ increased gradually, suggesting that the vortex was in the developing stage. After 17:40 JST, V_t and ζ began to decrease, and D began to increase, suggesting vortex decay. It is noted that Rankine fitness parameter, which is a standardized root-mean-squared difference between Doppler velocity field of Rankine vortex and that of the observed vortex, began to increase after the vortex began to decay (after 17:40 JST). This means that the velocity pattern of MGV was first well approximated by that of a Rankine vortex, but the deviation from Rankine vortex structure increased in its decaying stage.

3.2 *Misovortices embedded within MGV*

We investigated the behaviors of misovortices by single-Doppler analysis of RJRE. Lots of misovortices developed and decayed within MGV. Most of the long-lasting misovortices appeared in the northeastern part of the MGV, and moved cyclonically around the MGV center whereas MGV moved eastward (Fig. 4). The misovortices reached their maximum strength as they came into the northwestern part of the MGV (not shown).

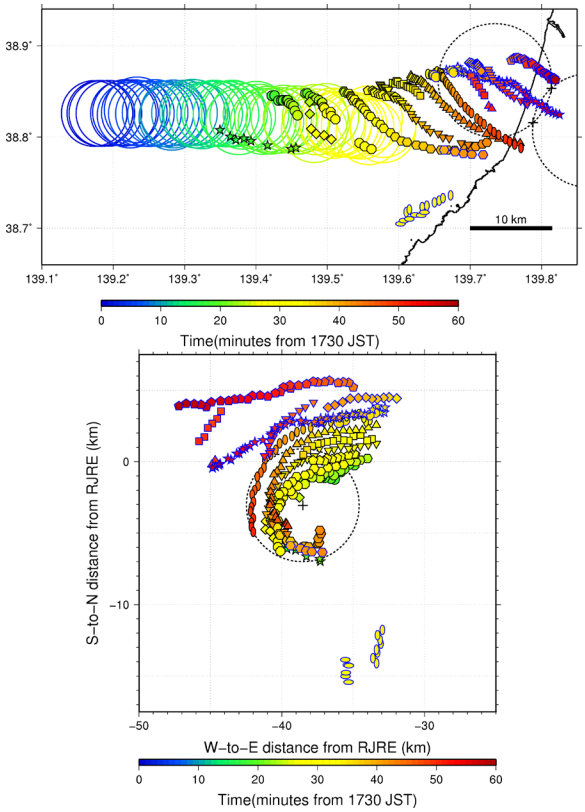

Fig. 4: (top) Tracks of MGV (colored open circle) and misovortices (color-filled symbols). Also shown are the area of dual-Doppler analysis (dashed circles), locations of radars (+), and coastline (solid line). (bottom) Tracks of misovortices relative to MGV center (+). Dashed circle represents a core radius of MGV at 17:45:42 JST. Colors represent minutes from 1730 JST.

The moving speed of the misovortices agreed well with the peak tangential velocity of MGV, suggesting that their movements were affected by the cyclonic rotation of MGV. It was also found that after MGV began to decay, the misovortices changed its moving direction and moved southeastward (Fig. 4).

Dual-Doppler derived wind field showed that the misovortices developed along the strong horizontal shear line in the northern part of MGV (Fig. 5). Some of the misovortices merged with nearby vortices as they develop. As they evolved, kinks in the reflectivity field also became pronounced. It is suggested that these misovortices were generated along the shear line that was produced by MGV circulation and that they developed by the horizontal shearing instability.

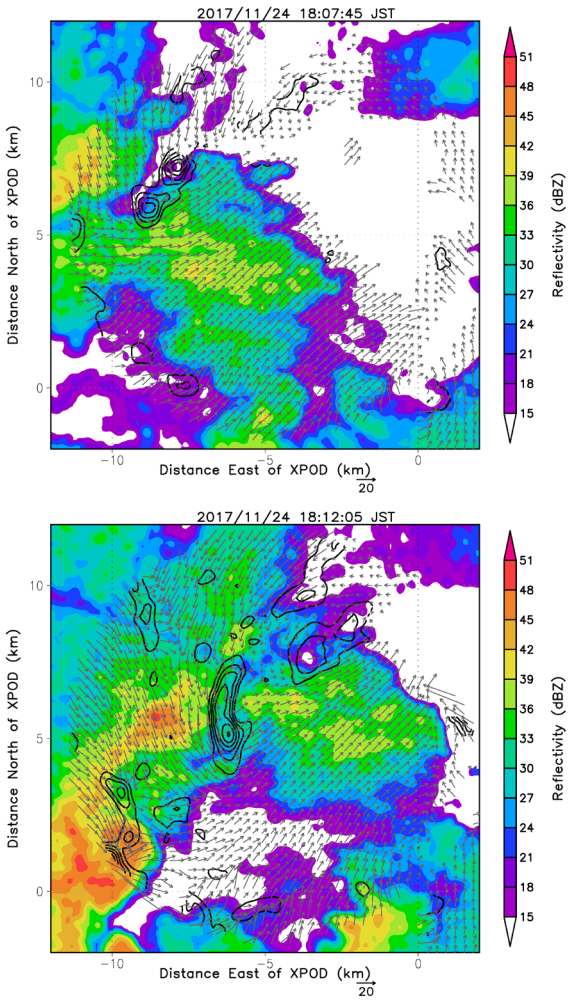

Fig. 5: Horizontal cross-section of RJRE reflectivity (shade), vertical vorticity (contours, outermost contour is 0.01 s^{-1}, incremented by 0.005 s^{-1}), and horizontal wind vectors at 300 m ASL at (top) 18:07:45 and (bottom) 18:12:05 JST.

4. CONCLUSION

To clarify the multi-scale structure of MGV observed on 24 November 2017, we performed single- and dual-Doppler analysis of MGV and misovortices embedded within it. The MGV developed offshore under a winter monsoon situation and approached the coast. It was first well approximated by a Rankine vortex with comma-shaped reflectivity pattern. As the misovortices developed within the MGV, MGV gradually decayed, and both Doppler velocity and reflectivity pattern became more complicated with small-scale velocity couplets and accompanying kinks. Most of the long-lasting misovortices appeared in the northeastern part of the MGV and moved cyclonically around the MGV center. They reached their maximum strength as they came into the northwestern part of the MGV. Dual-Doppler derived winds showed that the misovortices developed along the strong horizontal shear line within the MGV. It is suggested that the misovortices developed by the horizontal shearing instability and that their movements were affected by the cyclonic rotation of MGV.

References

Asai, T., 1988: Mesoscale features of heavy snowfalls in Japan Sea coastal regions of Japan. (in Japanese) *Tenki*, 35, 156–161.

Fujiwara, C., K. Kusunoki, H. Inoue, N. Ishitsu, K. Arai, and H. Suzuki, 2018: Development of train operation control method against gust using Doppler radar. Preprints, *10th European Conf. on Radar in Meteorology and Hydrology*.

Grim, J. A., N. F. Laird, and D. A. R. Kristovich, 2004: Mesoscale vortices embedded within a lake-effect shoreline band. *Mon. Wea. Rev.*, 132, 2269–2274.

Ishihara, M., Z. Yanagisawa, H. Sakakibara, K. Matsuura and J. Aoyagi, 1986: Structure of a typhoon rainband observed by two Doppler radars. *J. Meteor. Soc. Japan*, 64, 923-939.

Inoue, H. Y., and Coauthors, 2011: Finescale Doppler radar observation of a tornado and low-level misocyclones within a winter storm in the Japan Sea coastal region. *Mon. Wea. Rev.*, 139, 351–369.

Laird, N. F., L. J. Miller, and D. A. R. Kristovich, 2001: Synthetic dual- Doppler analysis of a winter mesoscale vortex. *Mon. Wea. Rev,* 129, 312–331.

Nagata, M., 1993: Meso-β-scale vortices developing along the Japan-Sea polar-airmass convergence zone (JPCZ) cloud band : Numerical simulation, *J. Meteor. Soc. Japan*, 71, 43-57.

Tsuboki, K., and T. Asai, 2004: The multi-scale structure and development mechanism of mesoscale cyclones over the Sea of Japan in winter, *J. Meteor. Soc. Japan*, 82, 597-621.

Suzuki, O., H. Yamauchi, M. Nakazato, and K. Akaeda, 2007: A new multi-scale meso-vortex / divergence detection algorithm with modified Rankine combined vortex, Preprints, *33rd Conf. on Radar Meteorology*.

Watanabe, S.I., H. Niino, and W. Yanase, 2016: Climatology of Polar Mesocyclones over the Sea of Japan Using a New Objective Tracking Method. *Mon. Wea. Rev.*, 144, 2503–2515

Yanase, W., H. Niino, S. I. Watanabe, K. Hodges, M. Zahn, T. Spengler, and I. A. Gurvich, 2016: Climatology of polar lows over the Sea of Japan using the JRA-55 reanalysis. *J. Climate*, 29, 419–437, doi:10.1175/JCLI-D-15-0291.1.